THE JOURNAL OF BIOLOGICAL CHEMISTRY VOL. 287, NO. 31, pp. 26352–26364, July 27, 2012

A Lectin from *Platypodium elegans* with Unusual Specificity and Affinity for Asymmetric Complex *N*-Glycans*[S]

Received for publication, April 25, 2012, and in revised form, June 7, 2012 Published, JBC Papers in Press, June 12, 2012, DOI 10.1074/jbc.M112.375816

Raquel Guimarães Benevides[‡§1], Géraldine Ganne[‡], Rafael da Conceição Simões[§], Volker Schubert[¶], Mathäus Niemietz[¶], Carlo Unverzagt[¶], Valérie Chazalet[‡], Christelle Breton[‡], Annabelle Varrot[‡], Benildo Sousa Cavada[‡2], and Anne Imberty[‡3]

From the [‡]Centre de Recherche sur les Macromolécules Végétales-CNRS (affiliated with Université Joseph Fourier and Institut de Chimie Moléculaire de Grenoble), 38041 Grenoble, France, the [§]Departamento de Bioquímica e Biologia Molecular, Universidade Federal do Ceará, Fortaleza, CE, 60.440-970, Brazil, and the [¶]Bioorganische Chemie, Gebäude NW1, Universität Bayreuth, 95440 Bayreuth, Germany

Background: Legume lectins with new glycan specificity can be discovered in the *Dalbergieae* tribe.
Results: We determined the sequence, specificity, and crystal structures of a new Man/Glc lectin (PELa) from *Platypodium elegans* seeds.
Conclusion: The unusual affinity of PELa for asymmetrical complex *N*-glycans is related to the extended binding site and conformational constraints on oligosaccharides.
Significance: *Dalbergieae* lectins are of interest for biotechnological applications.

Lectin activity with specificity for mannose and glucose has been detected in the seed of *Platypodium elegans*, a legume plant from the *Dalbergieae* tribe. The gene of *Platypodium elegans* lectin A has been cloned, and the resulting 261-amino acid protein belongs to the legume lectin family with similarity with *Pterocarpus angolensis* agglutinin from the same tribe. The recombinant lectin has been expressed in *Escherichia coli* and refolded from inclusion bodies. Analysis of specificity by glycan array evidenced a very unusual preference for complex type *N*-glycans with asymmetrical branches. A short branch consisting of one mannose residue is preferred on the 6-arm of the *N*-glycan, whereas extensions by GlcNAc, Gal, and NeuAc are favorable on the 3-arm. Affinities have been obtained by microcalorimetry using symmetrical and asymmetrical Asn-linked heptasaccharides prepared by the semi-synthetic method. Strong affinity with K_d of 4.5 μM was obtained for both ligands. Crystal structures of *Platypodium elegans* lectin A complexed with branched trimannose and symmetrical complex-type Asn-linked heptasaccharide have been solved at 2.1 and 1.65 Å resolution, respectively. The lectin adopts the canonical dimeric organization of legume lectins. The trimannose bridges the binding sites of two neighboring dimers, resulting in the formation of infinite chains in the crystal. The Asn-linked heptasaccharide binds with the 6-arm in the primary binding site with extensive additional contacts on both arms. The GlcNAc on the 6-arm is bound in a constrained conformation that may rationalize the higher affinity observed on the glycan array for *N*-glycans with only a mannose on the 6-arm.

Legume lectins compose a large family of homologous carbohydrate-binding proteins that are found primarily in the seeds of legume plants. Despite similarities in their physicochemical properties and their relatively conserved primary sequences, *Leguminosae* lectins display considerable diversity in their carbohydrate binding specificities, not only in terms of the recognition of monosaccharides but also in terms of differential binding to complex carbohydrates (1). Legume lectins are central to the study of the molecular basis and specificity of protein-carbohydrate interactions (2), and they also have technological implications for the understanding of cell-cell recognition, adhesion, tumor spread, bacterial and viral infection, and inflammation (3). However, the function of plant lectins remains elusive (4), although they are generally proposed to play a role in defense mechanisms against pathogens and invertebrate or vertebrate predators (5) or in the establishment of symbiosis (6). The mechanism of action still remains unclear even though induced response mechanisms are proposed for many pathogen-mediated injuries in plants. The direct interference with viruses and microorganisms is rather exceptional, but the deleterious effects of plant lectins on both predatory invertebrates and animals are well documented (5). The existence of hydrophobic sites within the structure of leguminous lectins, which bind phytohormones, suggests a possible role in certain aspects of hormonally regulated plant growth and development (7).

Leguminous plant lectins, although differing in carbohydrate-binding specificity, have similar amino acid sequences (1) and similar fold at the monomer level (8). The architecture of the so-called "legume lectin fold" is structurally related to a jelly roll motif characterized by a β-sandwich of 25–30 kDa that contains a carbohydrate-combining site, a tightly bound Ca^{2+}, and a transition metal ion, usually Mn^{2+}. Variability occurs both at the level of the quaternary fold, with a variety of dimeric and tetrameric arrangement (9), and at the level of the binding site. The floor of the binding site consists of few conserved key

* This work was supported in part by CNRS and the French Ministry of Research and the German Research Foundation (DFG).
[S] This article contains supplemental Figs. S1–S4 and Tables S1–S3.
The atomic coordinates and structure factors (codes 3ZVX and 3ZYR) have been deposited in the Protein Data Bank, Research Collaboratory for Structural Bioinformatics, Rutgers University, New Brunswick, NJ (http://www.rcsb.org/).
[1] Recipient of CAPES and CNPq grants from the Brazilian government.
[2] To whom correspondence may be addressed. E-mail: bscavada@ufc.br.
[3] To whom correspondence may be addressed. E-mail: imberty@cermav.cnrs.fr.

amino acids, but its perimeter depends on five loops with very variable size and sequence that control the carbohydrate specificity (8, 10, 11).

Lectins isolated from legume seeds have been regarded as a paradigm for investigating the structural basis and thermodynamics of selective sugar recognition (12, 13). The interaction between legume lectin and carbohydrate is generally characterized by a low affinity for monosaccharides (mM range). Longer oligosaccharides exhibit micromolar affinity, generally by generating a multivalent effect either by binding several sites of a multivalent lectin or by cross-linked neighboring lectins in solution (14, 15).

The large majority of leguminous lectins have been isolated and characterized from plants belonging to the *Phaseoleae* and *Vicieae* tribes of the *Papilionoideae* subfamily of Leguminosae (16). In this context, it would be of interest to characterize the structure and fine specificity of other lectins in different tribes to extend our knowledge on protein-carbohydrate interactions. The *Dalbergieae* tribe is of particular interest because only one lectin has been structurally characterized, *i.e.* the agglutinin from *Pterocarpus angolensis* seed (PAL).[4] Crystallography and thermodynamic studies demonstrated high affinity for both oligomannose *N*-glycans and for biantennary complex type, correlated with the presence of an unusually extended binding region close to the primary binding site (17–20).

In this study, we characterize the lectin from *Platypodium elegans* Vogel, another member of the *Dalbergieae* tribe. The genus *Platypodium* comprises two species of leguminous trees. *P. elegans* Vogel is a natural species found in the Brazil cerrado and in transition areas between cerrado and seasonal forest (21). We demonstrate here the presence of a mannose/glucose lectin (PELa) in *P. elegans* seeds. The cloning of the gene has been performed, resulting in the amino acid sequence determination of PELa. From the recombinant lectin, a complete study of the structure-specificity relationship has been performed, and we describe here the molecular basis of the unusual affinity of PELa for the asymmetric complex *N*-glycans.

EXPERIMENTAL PROCEDURES

Materials

P. elegans seeds were purchased from Reserva de Reflorestamento Flora Tietê (São Paulo, Brazil) and were stored at room temperature or at −70 °C. Monosaccharides, disaccharides, sulfated polysaccharides (Fucoidan, Carrageenan), and glycoprotein (pork stomach mucin) were purchased from Sigma.

Synthesis of Asn-linked N-Glycans H, E, and C

*Synthesis of **H***—Nonasaccharide-Asn **1** was prepared from egg yolk by enzymatic hydrolysis of its disialylated derivative (22). 10.0 mg (5.7 μmol) of nonasaccharide-Asn **1** were dissolved in 450 μl of phosphate buffer (100 mM, pH 6.8, 30 mM $MgCl_2$, 100 mM β-mercaptoethanol). To the solution were added 50 μl of buffered BSA (10 mg BSA/ml, 20 mM KH_2PO_4, 50 mM NaCl, 0.1 mM EDTA, pH 7). To this mixture 1 unit of lyophilized β-galactosidase (EC 3.2.1.23) was added. The mixture was incubated at 37 °C for 3 days (TLC: 2-propanol, 1 M ammonium acetate, 1.5:1). After lyophilization, the residue was dissolved in 500 μl of 0.1 M NH_4HCO_3 and purified by gel filtration (Superdex 30, 1.6 × 60 cm, 0.1 M NH_4HCO_3, 1 ml min^{-1}). The peak eluting at 80 min was lyophilized and desalted by gel filtration (Sephadex G-25, 2.5 × 70 cm, 5% ethanol in water, 0.5 ml min^{-1}). The peak eluting at 427 min was lyophilized yielding 5.2 mg of heptasaccharide-Asn **H** (64.1%). The purity was confirmed by 360 MHz ^1H NMR in D_2O.

*Synthesis of **E***—The Fmoc-protected octasaccharide-Asn **2** was isolated by HPLC according to Kajihara (22). 15.0 mg (8.3 μmol) of Fmoc-Asn(octasaccharide) **2** were dissolved in 320 μl of HEPES buffer (50 mM, pH 6.0, 0.1 mg ml^{-1} BSA). 17 μl (0.9 units) of a suspension of jack bean β-*N*-acetylglucosaminidase in 2.5 M $(NH_4)_2SO_4$, pH 7.0, were dissolved in HEPES buffer (50 mM, pH 6.0, 0.1 mg ml^{-1} BSA). The solutions of oligosaccharide **2** and the enzyme were combined, and the mixture was incubated at 37 °C for 3 days. After completion (LC-MS, C18, 20–35% MeCN (0.1% HCOOH)) the reaction was lyophilized. The residue was dissolved in 1 ml of 10% MeCN (0.1% HCOOH) and purified by RP-HPLC (NUCLEOGEL RP 100–10 (2.5 × 30 cm), 20–35% MeCN, 10 ml min^{-1}) The peak eluting at 29.3 min was lyophilized to yield 10.3 mg of Fmoc-Asn(heptasaccharide) **3** (77.3%). The purity was confirmed by LC-MS (C18, 20–35% MeCN (0.1% HCOOH)).

9.0 mg (5.6 μmol) of Fmoc-Asn(heptasaccharide) **3** were dissolved in a mixture of water, methanol, and acetonitrile (10:3:5). Subsequently, 89 μl (44.5 μmol) of sodium hydroxide (0.5 M) were added, and the solution was stirred for 3 h at ambient temperature. After completion (TLC: 2-propanol, 1 M ammonium acetate, 1.5:1), 850 μl of ammonium bicarbonate (0.1 M) were added, and the mixture was purified by gel filtration (Superdex 30, 1.6 × 60 cm, 0.1 M ammonium bicarbonate, 0.75 ml/min). The peak eluting at 108.2 min was lyophilized and desalted by gel filtration (Sephadex G-25 (2.5 × 71 cm), 5% ethanol in water, 0.5 ml min^{-1}). The fractions eluting at 422 min were lyophilized. Yield was 7.1 mg of **E** (5.1 μmol, 91.4%); R_f (*E*) = 0.31 (2-propanol, 1 M ammonium acetate, 1.5:1); $[\alpha]_D^{23} = +1.0$ (0.1, water); $C_{52}H_{87}N_5O_{38}$ (1390.26), ESI-MS negative mode: $M_{calc} = 1389.50$; $M_{found} = 1387.92$ $(M\text{-}H)^-$. The purity was confirmed by 360-MHz ^1H NMR in D_2O.

*Synthesis of **C***—11.0 mg (7.7 μmol) of heptasaccharide-Asn **H** were dissolved in 380 μl of HEPES buffer (50 mM, pH 6.0, 0.4 mg ml^{-1} BSA). 15.2 μl (0.81 units) of a suspension of jack bean β-*N*-acetylglucosaminidase (EC 3.2.1.52) in 2.5 M $(NH_4)_2SO_4$, pH 7.0, were dissolved in 50 μl of HEPES buffer (50 mM, pH 6.0, 0.4 mg ml^{-1} BSA). The solution of oligosaccharide **H** was added to the buffered enzyme, and the mixture was incubated at 37 °C for 5 days. After completion (ESI-MS), the reaction was lyophilized. The residue was dissolved in 0.3 ml of 0.1 M NH_4HCO_3 and purified by gel filtration (Superdex 30 (2.6 × 60 cm), 0.1 M NH_4HCO_3, 1.5 ml min^{-1}). The peak eluting at 149 min was lyophilized and desalted by gel filtration (Sephadex G-25 (2.5 × 71 cm), 5% ethanol in water, 0.5 ml min^{-1}). The elution at 451

[4] The abbreviations used are: PAL, *P. angolensis* lectin; ConA, concanavalin A; DGL, *D. grandiflora* lectin; ITC, isothermal titration calorimetry; LacNAc, *N*-acetyl-lactosamine; PELa, *P. elegans* lectin A; PSL, *P. sativum* lectin; TriMan, trimannose αMan1–3(αMan1–6)Man; RACE, rapid amplification of cDNA ends; Bicine, *N*,*N*-bis(2-hydroxyethyl)glycine; Fmoc, *N*-(9-fluorenyl)-methoxycarbonyl .

min was lyophilized to yield 3.7 mg of pentasaccharide-Asn **C** (46.8%). The purity was checked by 360 MHz ^{1}H NMR in D_2O.

Hemagglutination Tests on Seed Extracts

The seeds were ground and later defatted in the presence of *n*-hexane. A protein extract was prepared from 1 g of the ground seeds with 10 ml of 0.15 M NaCl at room temperature for 3 h. The homogenate was centrifuged at 16,000 × *g* for 20 min at 4 °C, and the precipitate was discarded. The hemagglutinating activity of the lectin was determined by a 2-fold serial dilution procedure using native rabbit or human erythrocytes as described previously (23). The hemagglutination titer was defined as the reciprocal of the highest dilution exhibiting observable hemagglutination. Inhibition of agglutination by sugar was assayed by serially diluting the solution of sugar in the microtiter plate, followed by the addition of four agglutinin units of the lectin and, after 30 min, of erythrocyte suspension. The lowest concentration of sugar that visibly decreased the extent of agglutination was defined as the minimum inhibitory concentration.

Cloning of PELa and Sequencing

For RNA isolation, 1 g of seeds was ground to a powder with a pestle under liquid nitrogen. Total cellular RNA was isolated using the Concert™ plant RNA reagent (Invitrogen), according to the manufacturer's protocol. Using the 3′-RACE kit from Invitrogen, mRNAs were converted into cDNA using reverse transcriptase and an oligo(dT) adapter primer. Partial cDNA of *P. elegans* seed lectin (*PELa*) was then obtained by PCR using a gene-specific primer (PLAT2, 5′-CAYATHGGNATHGAYGTNAA-3′) in combination with the abridged adapter primer of the 3′-RACE kit. PLAT2 was designed for minimal degeneration from a highly conserved peptide region (HIGIDVN) corresponding to the metal-binding site of legume lectins. The partial cDNA obtained was cloned into pGEM®T-easy (Promega) and sequenced. Complete coding region of *PELa* was obtained using the 5′-RACE kit (Invitrogen). mRNAs were first converted into cDNA using the antisense gene-specific primer PLAT3 (5′-TGATATAGAGATCCCTCTGGA-3′), which annealed downstream from the stop codon of *PELa,* and cDNA was then amplified using PLAT3 and the anchor primer of the 5′-RACE kit, after a TdT tailing step, and as described by the manufacturer. The PCR fragment was purified, cloned into the pGEM®T-easy, and further sequenced. All PCRs were performed using the GoTaq® DNA polymerase (Promega). The complete coding DNA sequence of *PELa* was then subcloned into the pET-29a plasmid (Invitrogen). PCR was performed using the 5′-RACE product as template and the sense PLAT4 (5′-GGAATTCCATATGCTACTGAATAGGGCAAAC-3′) and antisense PLAT5 (5′-GGCAAGCTTTCACATATCACGTGCAAGATAC-3′) primers, containing NdeI and HindIII restriction sites, respectively (underlined sequences). After digestion with NdeI and HindIII, the amplified fragment was introduced into the expression plasmid. The resulting plasmid was named pET-29a_PELa.

Expression and Purification of Recombinant PELa

Escherichia coli BL21(DE3) cells containing the plasmid pET-29a_PELa were cultured in LB broth medium at 37 °C. When the culture reached an A_{600} of 0.5–0.6, isopropyl β-D-thiogalactoside was added to a final concentration of 0.5 mM. Cells were harvested after 4 h of incubation at 30 °C, washed, and suspended in buffer A (50 mM Tris-HCl, pH 7.5, 150 mM NaCl, 5 mM $CaCl_2$, 5 mM $MnCl_2$). The cells were broken by cell disruption (Constant Cell Disruption System) at 1700 bars. After centrifugation at 20,000 × *g* for 30 min at 4 °C and filtration, the pellet was washed twice with 50 mM Tris-HCl, pH 8.0, 4 M urea, 0.5 M NaCl, 1 mM EDTA, 0.5% Triton X-100. The final precipitate was denatured and solubilized in 50 mM Tris-HCl, pH 8.0, 8 M urea, 10 mM DTT and, after centrifugation at 20,000 × *g* for 30 min at 4 °C, had its protein concentration adjusted to 1 mg ml^{-1}. 50 ml of the denatured protein solution at 1 mg ml^{-1} was slowly diluted in 950 ml of 50 mM Tris-HCl, pH 7.5, 240 mM NaCl, 2 mM $MnCl_2$, 2 mM $CaCl_2$, 10 mM KCl, 1 mM DTT. After 1 h at 10 °C and filtration, the fresh refolded protein was submitted to the purification step.

The purification of PELa was performed on a D-mannose-Sepharose column (Sigma). PELa refolded was allowed to bind to the immobilized mannose in equilibrating buffer (50 mM Tris-HCl, pH 7.5, 150 mM NaCl, 5 mM $CaCl_2$, 5 mM $MnCl_2$). After washing with buffer A, PELa was eluted using buffer A supplemented with 200 mM D-mannose. The purified protein was washed and concentrated as desired using a Vivaspin (Sartorius) ultrafiltration device with a cutoff of 10 kDa and stored at 4 °C. The protein fractions were analyzed on 12% SDS-PAGE, and the protein was stained with Brilliant Blue staining (Sigma).

Isothermal Titration Microcalorimetry Analysis

ITC experiments were performed with a VP-ITC isothermal titration microcalorimeter (Microcal; GE Healthcare). Experiments were carried out at 25 ± 0.1 °C. Protein was prepared in 50 mM Tris-HCl, pH 7.5, 150 mM NaCl, 5 mM $CaCl_2$, 5 mM $MnCl_2$, and the same buffer was used to prepare the oligosaccharide solutions. Protein (monomer) concentration used for ITC was 0.06 mM. Injections of 10 μl of each oligosaccharide solution at various concentrations (from 0.4 to 0.8 mM) were added automatically to the protein solution present in the calorimeter cell. Control experiments performed by injection of buffer into the protein solution yielded insignificant heat of dilution. Integrated heat effects were analyzed by nonlinear regression using a single site binding model (Origin 7.0) after subtracting the saturation heat evaluated at the end of the titration. The experimental data fitted to a theoretical titration curve gave the association constant (K_a) and the enthalpy of binding (ΔH). The other thermodynamic parameters such as changes in free energy (ΔG) and entropy (ΔS) were calculated from the equation $\Delta G = \Delta H - T\Delta S = -RT\ln K_a$, where T is the absolute temperature, and R is the molar gas constant (8.314 J·mol^{-1}·K^{-1}). All experiments were performed with c values of $10 < c < 100$, with c being the Wiseman constant (24) defined as $c = nK_a$ [M] ([M] receptor concentration in calorimeter cell).

TABLE 1
Data collection and refinement statistics

	Triman	Compound H
Beamline (wavelength)	Id14EH1/0.933 Å	BM30A/0.9797 Å
Space group	$P2_12_12_1$	$P2_12_12_1$
Cell dimensions *a, b, c*	42.62 80.68 148.76 Å	51.40 76.98 125.59 Å
α, β, γ	90.0, 90.0, 90.0°	90.0, 90.0, 90.0°
Resolution	42.60 to 2.10	47.57 to 1.65
(outer shell)	(2.21 to 2.10 Å)	(1.74 to 1.65 Å)
Measured/unique reflections	99,535/28,894	186,416/55,022
Average multiplicity	3.4 (2.4)	3.4 (2.6)
R_{merge}	0.082 (0.330)	0.054 (0.250)
Completeness	93.7% (70.1%)	91.4% (65.8%)
Mean $I/\sigma I$	9.3 (2.0)	13.6 (3.9)
Wilson B	24.7	14.00
R_{cryst}/R_{free}	19.5/25.2	15.5/18.8
r.m.s.d. bonds[a]	0.015 Å	0.015 Å
r.m.s.d. angles	1.54°	1.59°
r.m.s.d. chiral	0.106 $Å^3$	0.098 $Å^3$
Protein atoms	1935/1926	2004/1986
Bfac	23.5/23.7 $Å^2$	12.4/14.0 $Å^2$
Water molecules	177/149	295/223
Bfac	29.0/28.3 $Å^2$	25.7/26.6 $Å^2$
Ligand atoms	34	89/92
Bfac	22.6 $Å^2$	14.2/16.6 $Å^2$
Hetero atoms	18/8	30/12
Bfac, $Å^2$	32.4/33.5	24.7/25.7
Protein Data Bank code	3ZVX	3ZYR

[a] r.m.s.d. is root mean square deviation.

TABLE 2
Inhibition of hemagglutination activity of *P. elegans* seeds crude extract by various sugars

Sugars	Minimum inhibitory concentration
D-Mannose	12.5 mM
Methyl-α-D-mannopyranoside	6.12 mM
αMan1–2 Man	1.56 mM
αMan1–3 Man	1.56 mM
αMan1–6 Man	12.5 mM
D-Glucose	50 mM
Methyl-α-D-glucopyranoside	12.5 mM
Maltose	50 mM
N-Acetyl-D-glucosamine	25 mM
D-Galactose	–[a]
N-Acetyl-D-galactosamine	–
L-Fucose	–
D-Arabinose	–
Lactose	–
Lactulose	–
Fucoidan	–
Carrageenan	–
Pork stomach mucin	–

[a] No inhibition was observed at concentration of 100 mM.

Glycan Microarray Analysis

Purified PELa sample was labeled with Alexa Fluor 488 (Invitrogen) according to the manufacturer's instructions and re-purified on a D-Salt polyacrylamide desalting column (Pierce). Alexa-labeled protein was used for glycan array screening with a standard procedure of the protein-glycan interaction core (H) of the Consortium for Functional Glycomics.

Crystallization and Structure Determination

PELa was concentrated in 50 mM Tris-HCl, pH 7.5, 150 mM NaCl, 5 mM $CaCl_2$, 5 mM $MnCl_2$ to 10 mg ml^{-1} with addition of TriMan or compound **H** at the final concentration of 1 mM. Crystallization conditions for PELa were screened using the hanging-drop vapor diffusion method with a commercially available crystallization solution (Hampton Research Screens I and II, Hampton Research, Riverside, CA) at 20 °C. Drops were prepared by mixing a 1.0-μl sample solution and 1.0-μl reservoir solution, followed by equilibration against a 500-μl reservoir solution.

Crystals of the PELa-TriMan and PELa-heptasaccharide complexes were obtained using crystallization conditions 42 (1.5 M ammonium sulfate, 0.1 M Tris-HCl, pH 8.5, 12% v/v glycerol) and 48 (100 mM Bicine, pH 9, 10% PEG 20K and 2% dioxane) of the Crystal Screen II kit (Hampton Research), respectively. Crystals were frozen in liquid nitrogen (100 K) after soaking them for a time as short as possible in 25 and 30% (v/v) glycerol in precipitant solution, respectively. Data sets to 2.2 and 1.6 Å were collected for the PELa-TriMan and PELa-heptasaccharide complexes at European Synchrotron Radiation Facility (ESRF), Grenoble, France, on beamlines ID14-2 and BM30A, respectively, using an ADSC Q4R CCD (charge-coupled device) detector (Quantum Corp.). The statistics for both data collections are given in Table 1.

Phasing information was obtained using a monomer of *P. angolensis* lectin (Protein Data Bank code 1N3O, with removal of water molecules) as a probe for molecular replacement for the orthorhombic crystal form of the PELa-TriMan complex using the program PHASER (25). For the PELa-heptasaccharide complex, the crystal structure of the PELa-TriMan complex was used as template. Crystallographic refinement was carried out with the program REFMAC (26), and manual model building was achieved using Coot (27). Refinement statistics of both structures are given in Table 1. Coordinates have been deposited at the Protein Data Bank under code 3ZVX and 3ZYR, respectively. Molecular drawings were prepared using PyMOL Molecular Graphics System (DeLano Scientific, Palo Alto, CA) and LIGPLOT (28).

RESULTS AND DISCUSSION

Identification of Lectin Activity in P. elegans Seed Extracts

Crude extract from *P. elegans* seeds agglutinated rabbit erythrocytes with a titer of 2098 hemagglutination units ml^{-1}. Human erythrocytes with blood group A, B, and O were also tested, but no hemagglutination was observed. These results indicate the expression of at least one lectin in seeds with specificity for the oligosaccharides present in rabbit erythrocytes. Several monosaccharides and disaccharides were tested for their ability to inhibit PELa-induced rabbit erythrocyte agglutination as shown in Table 2. Glucose and its derivatives α-methylglucoside and GlcNAc demonstrated some inhibition, albeit at a rather large concentration. The most efficient compound is mannose, which could inhibit the agglutination at a concentration of 12 mM. Methyl-α-mannoside- and αMan-containing disaccharides are better ligands. These results indicate the presence of a mannose/glucose-binding lectin in the crude extract from *P. elegans* seeds.

RNA Isolation and cDNA Cloning

Total mRNAs were extracted from the seeds of *P. elegans,* and amplification of cDNA ends (3′-RACE and 5′-RACE) was performed using degenerated and specific primers. The specific degenerated primers were designed based on conserved peptide sequences known to be involved in binding to calcium and

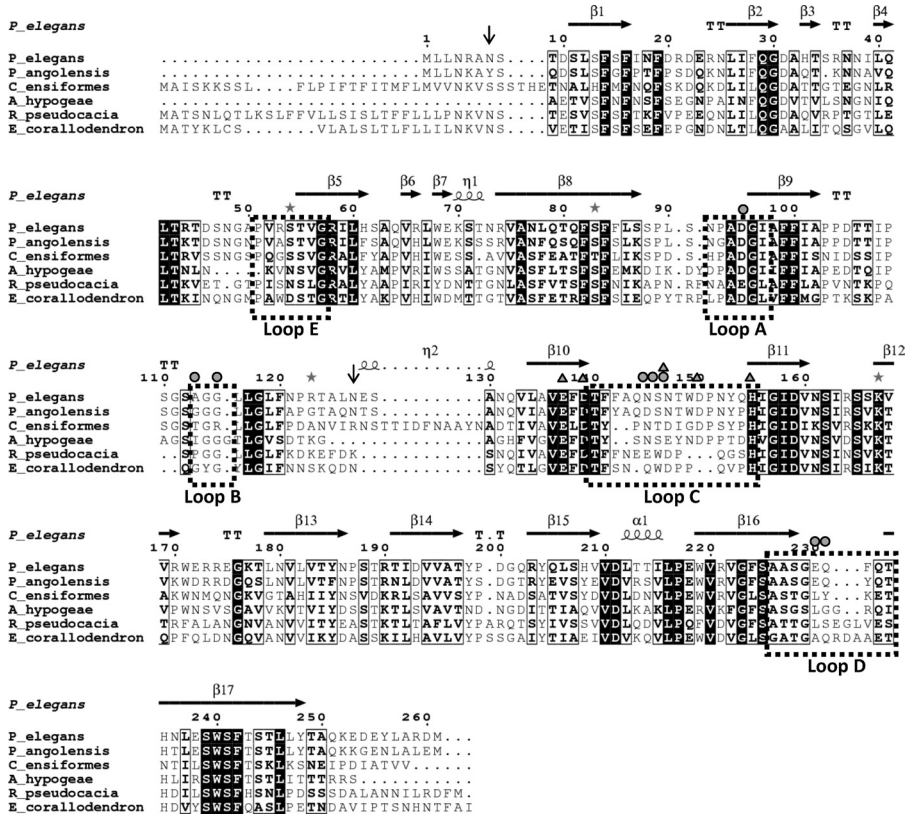

FIGURE 1. **Aligned amino acid sequences of legume lectins.** Multiple alignment and secondary structure predictions were achieved using the webESPript program (40). The sequence data were obtained from the Entrez protein sequence data base. ID numbers are as follows: AEK69351 (*P. elegans* lectin), CAD19804 (*P. angolensis* lectin), 2PEL_A (*A. hypogaea* lectin), CAA25787 (*C. ensiformes* lectin), BAA36415 (*Robinia pseudocacia* lectin), and CAA36986 (*E. corallodendron* lectin). Symbols are as follows: α-helices (α), 3_{10} helices (η), β-strands (β), strict α-turns (*TTT*), β-turns (*TT*), sugar binding residues (*circles*), metal-binding residues (*triangles*), and putative *N*-glycosylation sites ($\downarrow$).

manganese in legume lectins (supplemental Figs. 1S and 2S and supplemental Table 1S).[5]

The amino acid sequence deduced from the cDNA sequence indicates that the protein includes 261 amino acids with two predicted *N*-glycosylation sites (Asn-7 and Asn-127). PELa sequence shows similarities with other Man/Glc-specific legume lectins, such as those from *P. angolensis* (72% identity), *Pterocarpus rotundifolius* (82%), and *Arachis hypogaea* (70%) (ID numbers CAD19804, AAT57665, and AAA74572, respectively). Multiple alignment with a set of legume lectins with known crystal structures is displayed in Fig. 1. Sequence identities vary from 72% for the Man/Glc-specific lectin from *P. angolensis* to 39% for the Gal/GalNAc lectin from *Erythrina corallodendron*. The five loops that have been described to build the carbohydrate-binding sites (8, 10) are highlighted in Fig. 1. Sequences in these loops present strong similarities with *P. angolensis* lectin, but weaker similarities with other lectins, in agreement with the large differences in monosaccharide specificities.

Expression and Purification of Recombinant PELa

Production of recombinant PELa in *E. coli* BL21(DE3) strain resulted in the accumulation of the protein in inclusion bodies. A renaturation protocol, including solubilization by 8 M urea, was used to obtain the protein in the soluble form (supplemental Fig. 3S). Active PELa was obtained by affinity purification on a mannose-agarose column with a final yield of 5 mg of PELa/liter of cell culture. The soluble lectin displays a molecular mass of 29 kDa, in agreement with the theoretical one (29.287 kDa). The activity of the lectin was checked at each step of production and purification by hemagglutination assay.

Specificity of PELa

The lectin specificity was analyzed by glycan array (Consortium for Functional Glycomics) that allows the screening of a broad spectrum of natural and synthetic glycans. The printed array version 4.1 containing 465 natural and synthetic glycans was used, and PELa was observed to bind to a limited number of oligosaccharides (Fig. 2*A*). Short oligosaccharides are not bound with the exception of linear or branched oligomannose fragments (compounds **A** and **B**). The lectin is specific for *N*-glycans. Oligomannose-type *N*-glycans with terminal nonreducing α-mannose are high affinity ligands (compounds **C** and **D**). However, the lectin displays a clear preference for asymmetrical complex-type *N*-glycans with a short 6-arm, containing only the αMan residue, and long 3-arm with *N*-acetyl-lactosamine (LacNAc) (compound **E**) or sialylated LacNAc (compound **F**) on the αMan residue. Symmetrical complex *N*-glycans are not bound in the same way. The truncated complex *N*-glycan terminated by two GlcNAc residues (compound **H**) is recognized, albeit more weakly than the asymmetrical

[5] RNA and protein sequences have been deposited GenBank with codes JN133278 and AEK69351, respectively.

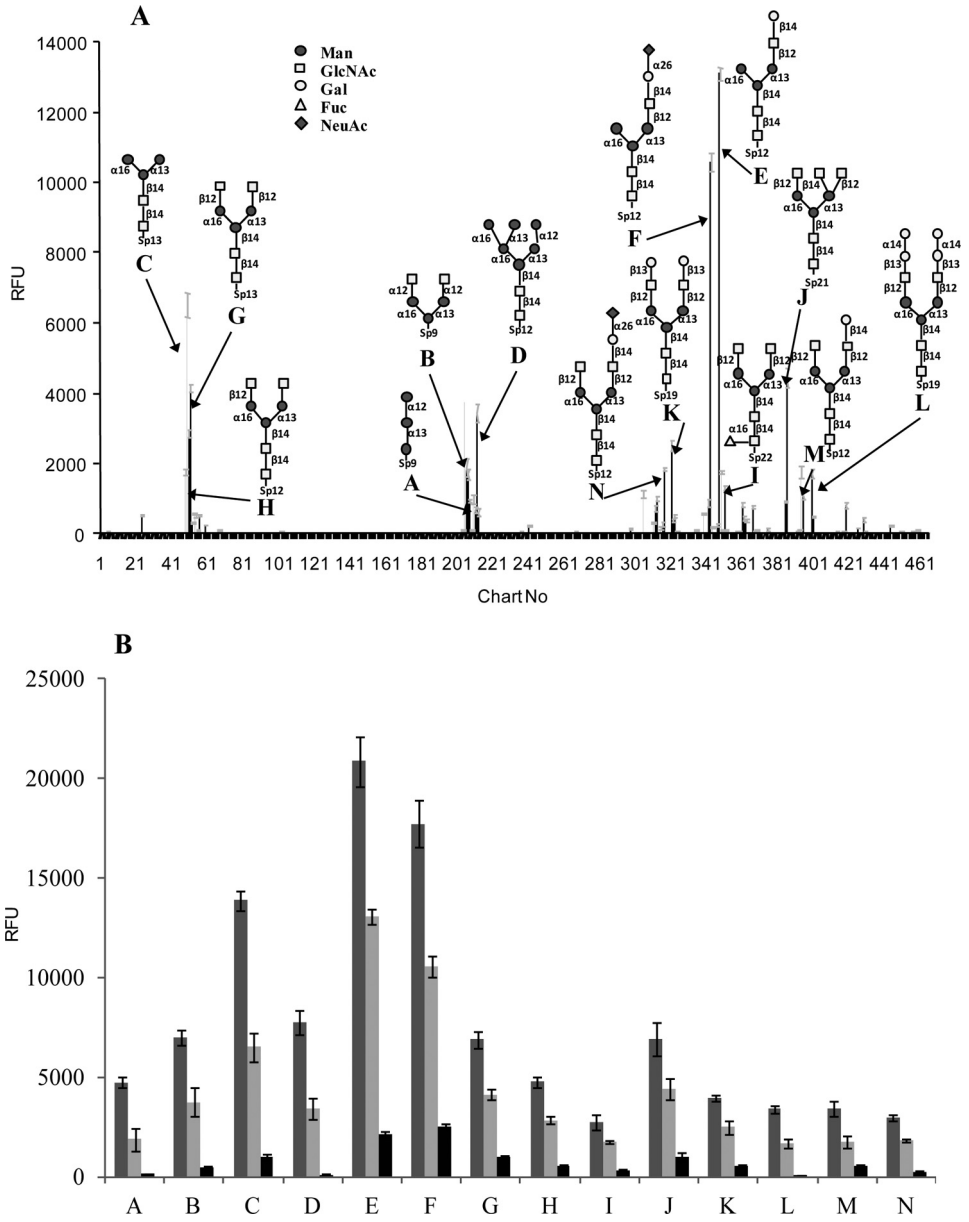

FIGURE 2. **Glycan array data.** *A,* binding of labeled PELa (10 μg ml^{-1}) to all carbohydrates of the glycan array version 4.1. *B,* comparison for binding at three lectin concentrations (*medium gray,* 50 μg ml^{-1}; *light gray,* 10 μg ml^{-1}; *dark gray,* 1 μg ml^{-1}).

compounds. In contrast, the more complete complex *N*-glycans terminating with *N*-acetyllactosamine (LacNAc, βGal1-4GlcNAc) or sialyl-LacNAc are not recognized. Interestingly, the same compounds with a β1–3 linkage between Gal and GlcNAc are bound (compounds **K** and **L**), albeit less strongly than the asymmetrical compounds.

Glycan array results allowed a semi-quantitative analysis by reporting the intensities of fluorescence at different protein concentrations. As displayed in Fig. 2*B*, the preference for asymmetrical complex *N*-glycans is conserved for the three PELa concentrations tested (50, 10, and 1 μg ml^{-1}) of lectin. The influence of the terminal sialic acid on the 3-arm seems to be moderate because oligosaccharides **E** and **F** have a rather equivalent response at low protein concentration. Comparing the concentration-dependent fluorescence response between oligosaccharides **E** and **M**, and also **F** and **N**, clearly confirms that the addition of one GlcNAc on the 6-arm significantly decreases the lectin affinity.

Glycan array data for other legume lectins are available on line. The classical Glc/Man legume lectins such as ConA from *Canavalia ensiformis* and lectin from *Pisum sativum* bind preferentially to oligomannose-type *N*-glycans, more weakly to complex *N*-glycan, and not much to asymmetrical *N*-glycans. These data therefore demonstrate that the unusual specificity of PELa for asymmetrical glycans is clearly different from the classical Glc/Man legume lectins.

Synthesis of Symmetrical and Asymmetrical Asn-linked N-Glycans

The *N*-glycan asparagines **H** and **E** were both obtained by chemical and enzymatic conversion of a sialoglycopeptide isolated from egg yolk (Scheme 1) (29). The nonasaccharide-Asn **1**

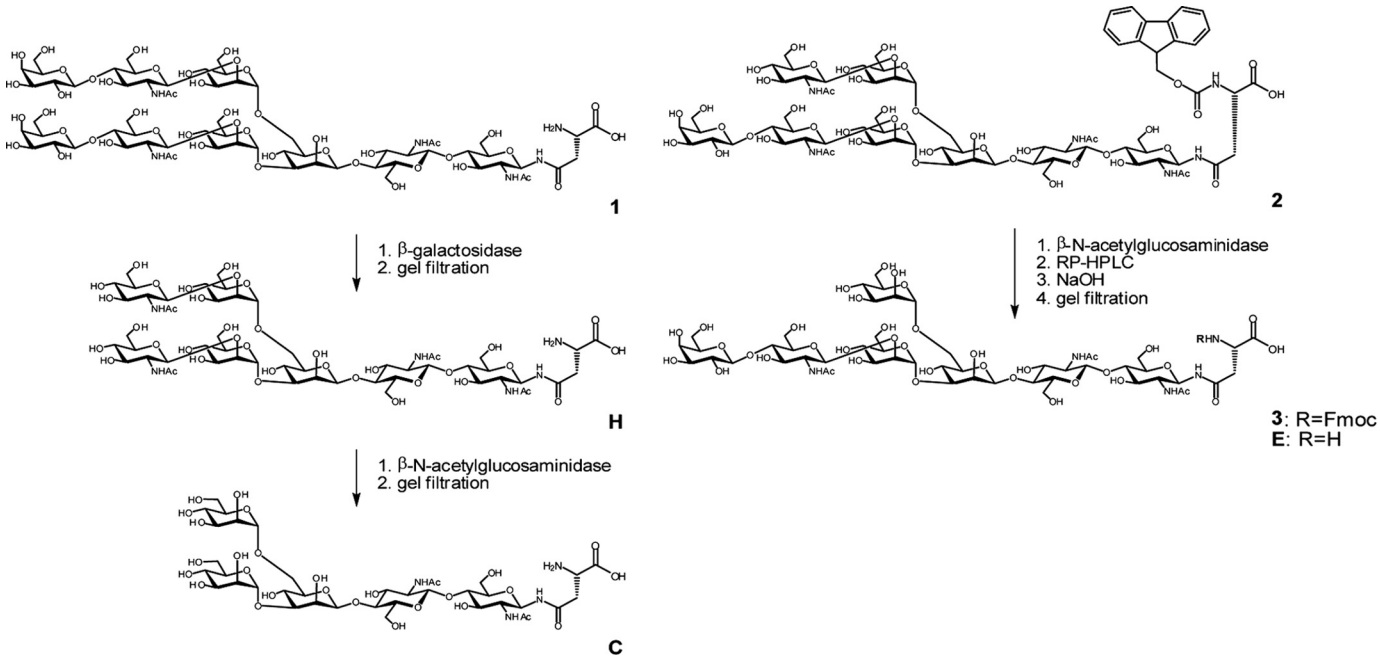

SCHEME 1. **Schematic representation of glycopeptide synthesis.**

(22) was prepared from the Fmoc-protected precursor according to a previously disclosed procedure (30). Removal of both terminal galactosyl moieties was accomplished by digestion with *E. coli* β-galactosidase followed by purification and desalting via gel filtration. The heptasaccharide-Asn **H** (22, 31) was obtained in good yield and high purity. For the preparation of asymmetrical compound **E**, the purification of a suitable precursor was carried out using a mixture of Fmoc-protected *N*-glycan asparagines. According to Kajihara (22), the separation of Fmoc octasaccharide-Asn **2** (terminal galactoside on the 3-arm) from its isomer (galactoside on the 6-arm) can be performed by preparative HPLC. Compound **2** was digested with jack bean β-*N*-acetylglucosaminidase and purified by RP-HPLC yielding as an intermediate the Fmoc-protected heptasaccharide-Asn **3**. Alkaline cleavage of the Fmoc group led to the target compound **E**. The pentasaccharide-Asn **C** was obtained from heptasaccharide-Asn **H** using jack bean β-*N*-acetylglucosaminidase. The ^{1}H NMR resonances of the sugar part of compounds **1**, **2**, **3**, **H, E,** and **C** (supplemental Fig. 4S) were in accordance with the published data (22). Depending on the pH and on counter ions, the resonances of the Asn moiety may vary.

Affinity Measurements by Titration Microcalorimetry

The affinity between PELa and the three Asn-linked oligosaccharides **C**, **E**, and **H** was estimated by titration microcalorimetry by injecting aliquots of ligands in the cell containing the protein, and the resulting thermograms are displayed in Fig. 3. In all cases, strong exothermic peaks are observed indicating a favorable enthalpy of binding as classically observed in protein-carbohydrate interactions (13). No precipitation was observed at the end of titration. Using a simple one site model, oligosaccharides **E** and **H** bind with similar affinities, with K_d of ~5 μM. Such affinity is unusually strong for legume lectins and has been obtained only for trimannoside in multivalent binding to ConA or *Dioclea grandiflora* lectin (DGL) (14, 15). The shorter glycopeptide **C** (pentasaccharide-Asn) presents a lower affinity (K_d = 185 μM) in agreement with glycan array data. In the case of the symmetrical glycan **H**, a better fit is obtained using a model with two sites indicating that each branch of the heptasaccharide can bind to the lectin but with different affinities. However, no quantitative data can be safely extracted when using a two sites model for fitting procedure. In contrast, the unsymmetrical glycan **E** fits very well with the one site model.

As displayed in Fig. 3, the heat released by oligosaccharides **H** and **E** when binding to PELa are very different, as well as the shape of the peaks. Longer time is required for oligosaccharide **H** to come to equilibrium. Although both compounds have approximately the same affinity for PELa, and therefore similar free energy of binding ΔG of about -30 kJ mol^{-1} (Table 3), the enthalpy and entropy contributions are very different. The symmetrical compound **H** has a medium size enthalpy of binding ($\Delta H = -23$ kJ mol^{-1}) and a favorable entropy that contributes to ~20% of the binding energy ($-T\Delta S = -7.2$ kJ mol^{-1}). The asymmetrical compound **E** has a much higher enthalpy of binding ($\Delta H = -54$ kJ mol^{-1}) and a strong entropy barrier with an unfavorable contribution of $-T\Delta S = 23$ kJ mol^{-1}. Compound C (pentasaccharide-Asn) binding is also enthalpy-driven (Table 3). In relation to the presence of an additional GlcNAc on the 6-arm, compound **H** therefore has a different behavior, with longer equilibrium time related to favorable entropy of binding.

Crystal Structures of PELa in Complex with Oligosaccharides

Overall Description—Crystals for different complexes were obtained by the hanging drop vapor diffusion method. The protein at 10 mg ml^{-1} was incubated with 1 mM oligosaccharide prior to testing crystal growth. Co-crystallization with the branched trimannose αMan1–3(αMan1–6)Man (TriMan) leads to crystals diffracting to 2.1 Å in space group $P2_12_12_1$

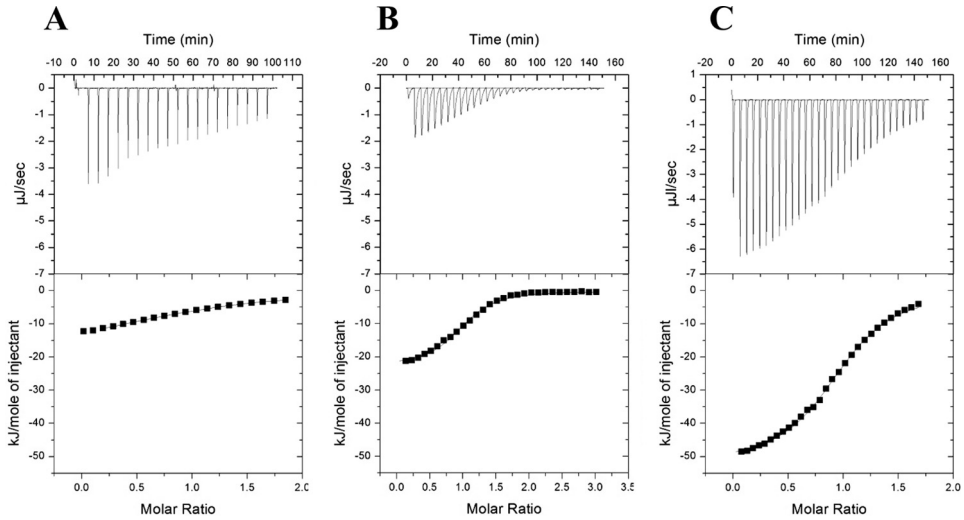

FIGURE 3. **Microcalorimetry data.** ITC plot obtained from the titration of PELa (60 μM) by Asn-linked glycans **C** (*A*), **H** (*B*), and **E** (*C*) measured on ITC200 (*A*) and VP-ITC (*B* and *C*) from Microcal. The plots in the *lower panel* show the total heat released as a function of total ligand concentration for the titration shown in the *upper panels*. The *solid line* represents the best least squares fit to the experimental data using a one site model.

TABLE 3

Microcalorimetry titration data for the binding of the oligosaccharides E and H to PELa

All measured values are averaged over two experiments except for compound C. Standard deviations are indicated in parenthesis.

Ligand	K_d	n	$-\Delta G$	$-\Delta H$	$-T\Delta S$
	μM		*kJ/mol*	*kJ/mol*	*kJ/mol*
Compound **H**	4.6 (0.3)	1.06 (0.06)	30.4	23.2 (0.3)	−7.2
Compound **E**	4.5 (0.2)	0.98 (0.06)	30.5	53.9 (1.8)	23.4
Compound **C**[a]	133	1.03	22.1	18.7	−3.4

[a] Performed on ITC200.

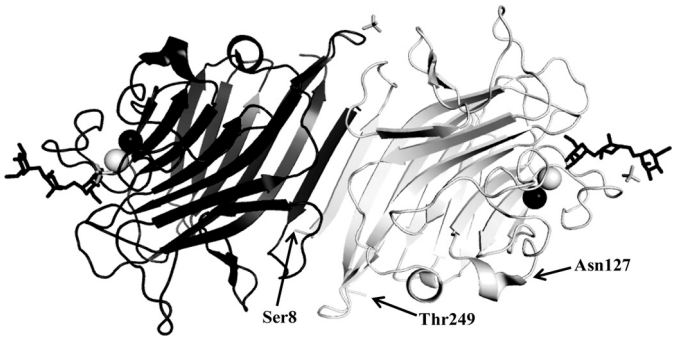

FIGURE 4. **Overall structure of a dimer of PELa complexed with trimannoside.** Peptide chains are represented as ribbon colored in *light gray* (chain A) and *dark gray* (chain B). Oligosaccharides are represented by *sticks* and calcium and manganese ions by *white* and *black spheres*, respectively.

(Table 1). The structure was solved by molecular replacement using the coordinates of PAL (Protein Data Bank code 1N3O). A dimer of lectin and one molecule of ligand are observed in the asymmetric unit. Crystals were also obtained with the symmetrical glycan **H**, diffracting to 1.6 Å in the same space group but with a different unit cell. The structure was solved by molecular replacement using the coordinates of the PELa-TriMan complex. A lectin dimer and two oligosaccharides are observed in the asymmetric unit.

In both structures, each monomer of PELa adopts the classical β-sandwich fold observed in all legume lectins, with the presence of one calcium and one manganese ion (Fig. 4) (9). From the 261 residues of PELa, all could be identified in the electron density map, except for the first 7 or 8 at the N-terminal extremity, and the last 11 to 12 at the C-terminal extremity, depending on the chain. The two monomers in the asymmetric unit associate by parallel arrangement of their back β-sheet, resulting in the "canonical legume lectin dimer" that is classically observed in both dimeric and tetrameric legume lectins (9). The two potential glycosylation sites Asn-7 and Asn-127 are located in the disordered N-terminal region and in the loop at the surface of the protein, respectively (Fig. 4). Both positions are therefore likely to be glycosylated in plants.

Crystal Structure of PELa-Trimannose Complex—The complex of the lectin with TriMan contains very clear density for the trisaccharide bridging two symmetry related PELa dimers, resulting in formation of lectin chains in the crystal (Fig. 5, *A* and *B*). The two α-linked mannose residues are bound in facing monomers, the 1–3 linked mannose in monomer A and the 1–6 linked one in monomer B. The binding modes of the two mannose residues are very similar, each establishing five direct hydrogen bonds with side chains of Asp-95, Asn-147, and main chain nitrogen of Gly-115 and Glu-230 (Fig. 5*C*). Hydrophobic contacts involve Ala-94 and Phe-141. This interaction corresponds to the classical mannose binding mode observed in PAL (20) and ConA (32). A conserved water bridge was also observed at both sites between O2 and the carbonyl oxygen of Ala-113.

The central core mannose residue establishes bonds with both monomers, involving Asn-145, Ser-146, and Gln-231 of chain A and Glu-230 of chain B. The bridging TriMan results in rather close contact of the two facing protein monomers. Protein-protein contacts are created with the participation of Arg-123B side chain hydrogen bonded to Thr-148-A and Asp-150-A main chain. Also, the Asn-145 residue of each monomer interferes with the binding site of the other monomer and participates in hydrogen bonding to mannose O2 for Asn-145B or in hydrophobic contact to C2 for Asn-145A (Fig. 5, *B* and *C*). Because of the different environments, Asn-145 side chains of the two monomers have different orientations, and the back-

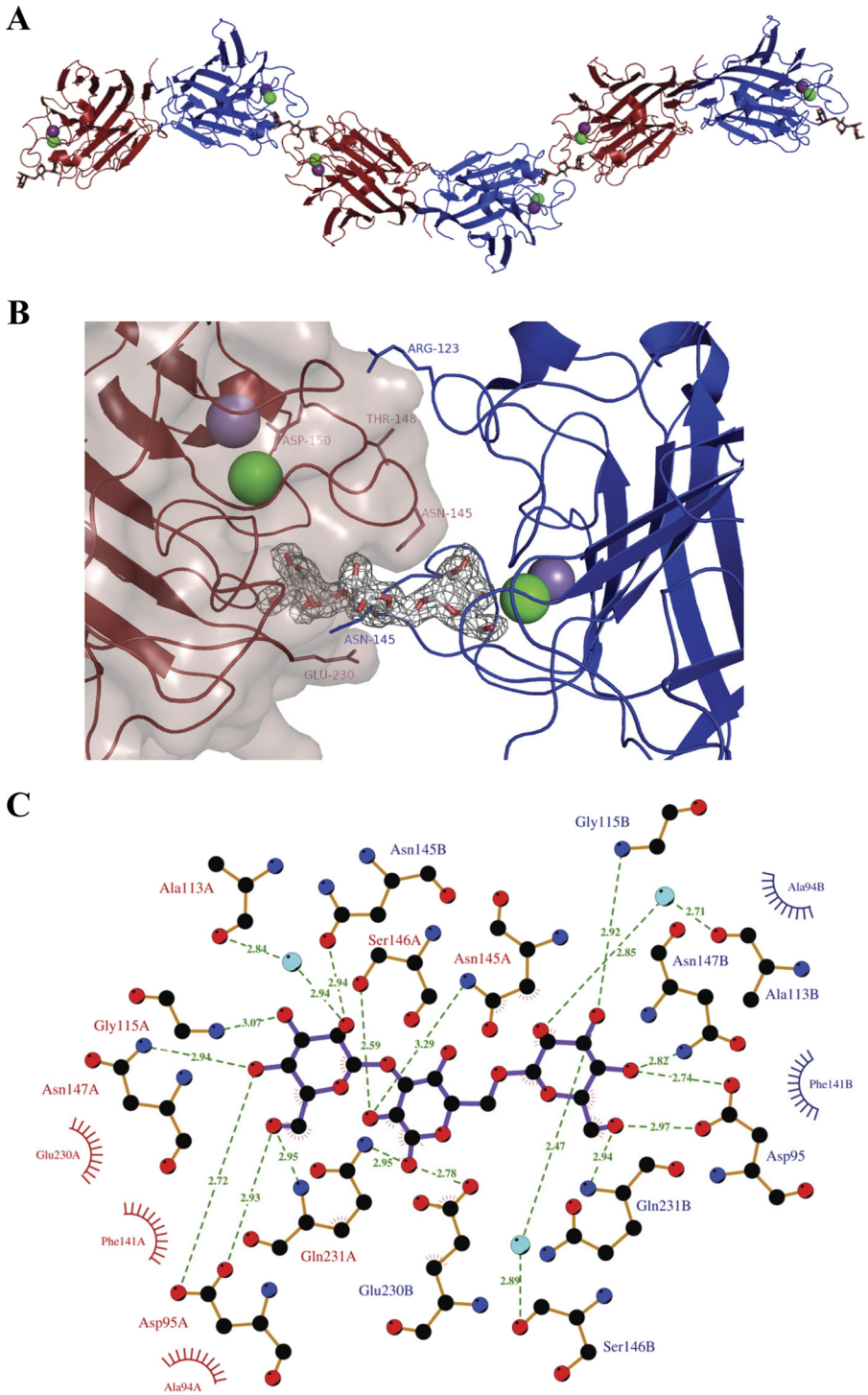

FIGURE 5. **Crystal structure of PELa-trimannoside complex.** *A,* chains of PELa lectins bridged by trimannosides represented as ribbons colored in *red* (chain A) and *blue* (chain B). *B,* close view of the interface with the trimannoside represented together with its $2mF_o - DF_c$ electron density maps contoured at 1 σ (0.32 electrons per Å^3). Chain A is represented by its accessible surface (*red*) and chain B as ribbon (*blue*). *C,* LIGPLOT representation of the hydrogen bonds and van der Waals contact around the trimannoside.

bone of loop C also displays slightly different conformations (Fig. 6*A*).

As a result of its interaction with facing monomers, the TriMan shape is very extended and differs from what has been previously observed in other complexes with legume lectins such as PAL (20), ConA (33), and DGL (34). Comparison between PELa and PAL confirms the strong similarity between the binding sites, with same conformation of the five loops, labeled A–E (Fig. 6*A*). PAL binds the trimannoside with the αMan residue of the 6-arm in the primary binding site, as in monomer B of PELa. Nevertheless, the observed oligosaccharide conformation is very different because TriMan folds around the phenyl residue in the binding site of PAL, and the 3-linked mannose is hydrogen bonded to an asparagine residue

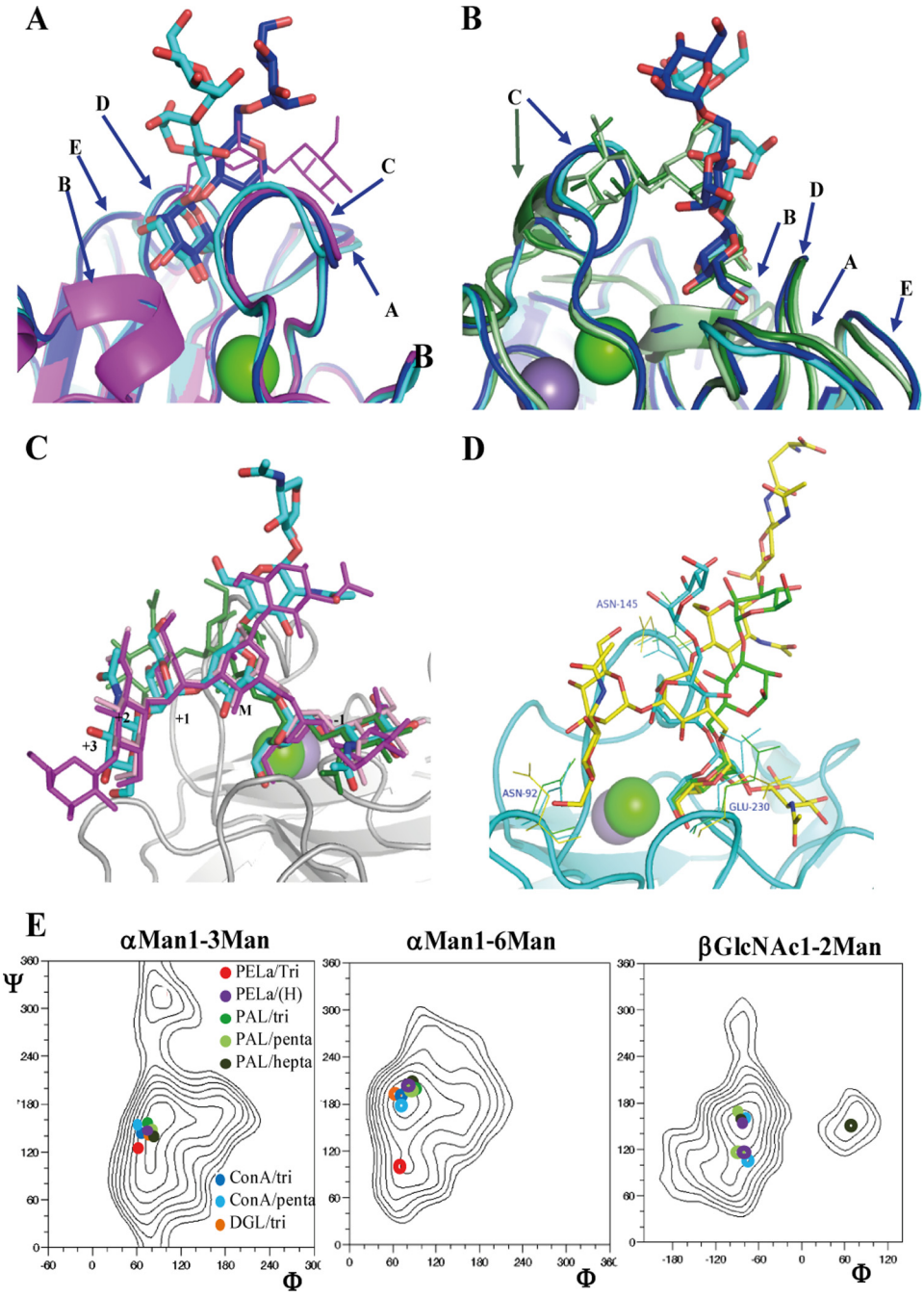

FIGURE 6. **Comparison of PELa-oligosaccharide complexes with related ones from other legume lectins together with labeling of loops from the binding site and analysis of the conformation of oligosaccharides bound to PELa.** *A,* superimposition of chain A (*blue*) and chain B (*cyan*) from the PELa-trimannoside complex together with PAL-trimannoside structure (*magenta,* Protein Data Bank code 1Q8V) (20). *B,* orthogonal view for chains A and B of PELa together with trimannoside complexed with ConA (*dark green,* 1ONA) (33) and with *D. grandiflora* lectin (*light green,* 1DGL) (34). *C,* superimposition of chain B (*cyan*) from PELa-Asn-linked heptasaccharide complex with complex oligosaccharides in the crystal of PAL (*magenta,* 2ARX; *salmon,* 2A6X) (17) and ConA (*green,* 1TEI) (36). *D,* comparison of the three binding modes observed in crystal structures as follows: TriMan bound through the αMan1–3 (*cyan*) and by the αMan1–6 (*green*) residues and heptasaccharide-Asn (*yellow*). *E,* energy maps are from 3D-cermav. Conformation at each linkage of all complexes has been superimposed on the corresponding energy map. *Open* and *filled circles* represent conformations of the 6-arm and 3-arm, respectively.

in loop A. The difference in conformation of TriMan in PELa and PAL is due to a 90° shift in the Ψ dihedral angle of the αMan1–6Man linkage, the unusual value of 105° observed in PELa complex (Fig. 6*E* and Table 4) resulting in the extended shape of TriMan. Comparison with lectins from the *Dioclae* tribe is displayed in Fig. 6*B*. Binding site loops are well conserved between *Dioclea* (ConA and DGL) and *Dalbergieae* (PAL and PELa), with the exception of loop C that is shorter in ConA/DGL than in PAL-PELa (14 amino acids instead of 16) resulting in a more open binding site, as described previously (20). As a result, the TriMan conformation in ConA and DGL is different; it folds back on the protein surface and the 1–3-linked α-Man makes additional contact with amino acids of loop C. The conformation observed for TriMan in ConA could not be possible in PELa due to the different conformation of loop C that would result in a steric conflict.

TABLE 4

Torsion angles (Φ,Ψ) or (Φ,Ψ,ω) at selected glycosidic linkages in the crystal structures of PELa-oligosaccharide complexes and other lectins displayed in Fig. 6

All values are given in degrees. $\Phi = \theta(O5–C1–O1–Cx')$, $\Psi = \theta(C1–O1–Cx'–Cx_{+1}')$, $\omega = \theta(O1–C6—C5'–O5')$.

	1–6 arm		1–3 arm	
	αMan1–6Man	βGlcNAc1–2Man	αMan1–3Man	βGlcNAc1–2Man
PELa-trimannose[a]	70, 105, −53		65, 123	
PAL-trimannose	92, −149, −56		70, 129	
ConA-trimannose	75, −171, −63		72, 119	
DGL-trimannose	64, −165, −46		63, 129	
PELa-heptaose-Asn (H)	90, −153, −57	−79, 115	69, 128	−85, 152
PAL-pentaose	89, −154, −55	−81, 115	70, 129	−90, 170
PAL-heptaose	84, −147, −56	76, 150	72, 130	−84, 167
ConA-pentaose	68, 175, −43	−71, 105	62, 137	−80, 157

[a] See legend of Fig. 6 for Protein Data Bank code. A representative chain has been selected in each structure.

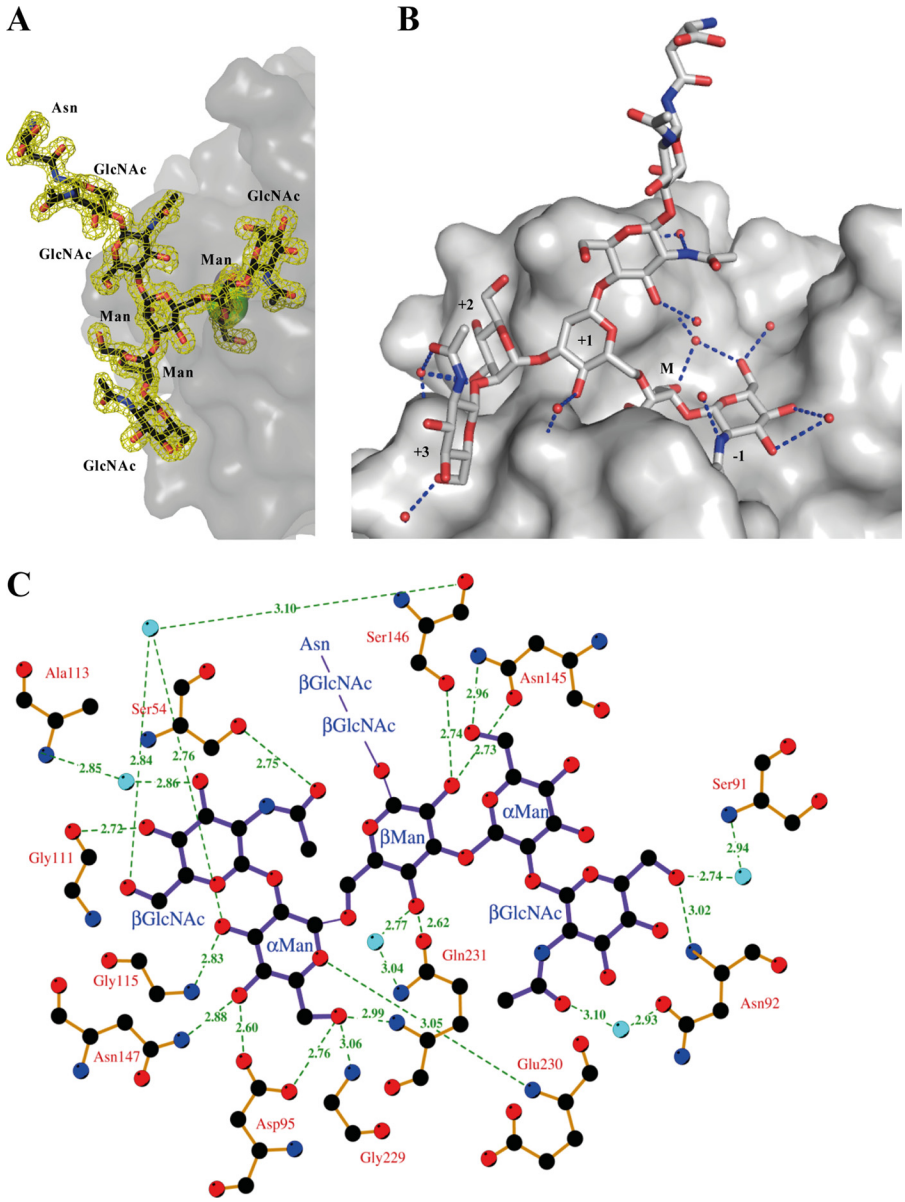

FIGURE 7. **Crystal structure of PELa-compound H complex.** *A*, $2mF_o - DF_c$ electron density maps contoured at 1σ (0.47 electrons per Å^3) around the heptasaccharide-Asn in monomer A. *B*, representation of the oligosaccharide on the protein surface. *C*, LIGPLOT representation of the hydrogen bonds for the ligand in monomer A. The chitobiose and asparagine moiety do not establish hydrogen bond with the protein, and for the sake of clarity, they are not displayed in the figure.

PELa-Asn-linked Heptasaccharide Complex—Clear density for the whole biantennary heptasaccharide was observed in both monomers of PELa, and the linked asparagine residue could be located in monomer A (Fig. 7*A*) because of its stabilization by a salt bridge with Arg-221 of a symmetry-related protein. Apart from this slight difference, the oligosaccharides in

chains A and B are very similar in terms of conformation and hydrogen bonds (details available in supplemental Tables 2S and 3S), and all descriptions below will refer to monomer A, unless otherwise indicated. The mannose of the 6-arm is located in the primary binding site (subsite M) with the same orientation and the same hydrogen bond network as described above for the TriMan ligand. With the exception of the asparagine and the first GlcNAc attached to it, all residues are interacting with the protein surface, resulting in an extended surface of contact (Fig. 7*B*). The second GlcNAc of the chitobiose core sits against loop C and establishes a water-bridged hydrogen bond with Asn-145 main chain oxygen. The numerous other contacts involve both arms of the biantennary glycans. The GlcNAc on the 6-arm establishes three hydrogen bonds with amino acids of site −1 (Fig. 7*C* and supplemental Table 3S). The core mannose in site +1 and the 3-arm in sites +2 and +3 also displays a large number of contacts. Altogether, more than 15 direct hydrogen bonds and 6 water-bridged ones are observed, rationalizing the high affinity measured by titration microcalorimetry.

The conformations of the oligosaccharides have been analyzed and compared with previously determined energy maps (35). The conformation of the βGlcNAc1–2Man and αMan1–3Man linkages in the 3-arm are close to the global minima (Table 4 and Fig. 6*E*). For the other antenna, the αMan1–6Man linkage is in a low energy conformation, with a GG conformation of the ω angle, but the βGlcNAc1–2Man linkage is clearly distorted with a Ψ value of about 115°, in a region of the energy map that is 4 kcal mol^{-1} above the global minimum at Ψ = 150°. It could be noted that the O3 oxygen atom of this GlcNAc is solvent-exposed and available for elongation by a Gal residue, although the O4 points toward the Ser-110–Gly-111–Ser-112 peptides close to loop B and cannot be substituted. This is in agreement with glycan array data showing no binding to symmetrical *N*-glycans with LacNAc on both arms.

The conformation of the biantennary glycan and the network of contacts are very similar to what has been described previously for the structure of PAL interacting with complex-type pentasaccharide (17), albeit with small differences at the extremities of branches (Fig. 6*C*). The same pentasaccharide complexed with ConA exhibits the same position of 6-arm in subsite M and −1, but a different orientation of the 3-arm, again because of the important difference in loop C conformation (36). The same distorted orientation of the βGlcNAc1–2Man linkage in subsite −1 was described for the ConA complex. It should be noted that in other complexes, such as PAL-heptasaccharide (17), this linkage adopts a completely different orientation with a large change in the Φ angle (Fig. 6*E*).

CONCLUSION

This study describes a very complete sequence/structure/specificity characterization of a legume lectin from the *Dalbergieae* tribe with unusual affinity for asymmetric complex *N*-glycans. The sequence and structure present similarity with the lectin from *P. angolensis*, PAL, the only *Dalbergieae* lectin that was structurally characterized previously (17–20). Some of the structural features of binding of PELa to complex *N*-glycans are also common to both lectins, such as the occurrence of an extended binding site that results in a very large surface of contact between the oligosaccharide and the protein. Nevertheless, very important new data are revealed by this work. This is the first characterization of a lectin from this subfamily by glycan array. Interestingly, PELa binds to a subset of complex *N*-glycans, and this binding profile is very different from those already determined for other lectins with Glc/Man specificity such as ConA, DGL, and lectins from *P. sativum* and from *Lens culinaris* that all bind preferably to oligomannose type *N*-glycans. We could also determine the very high affinity of PELa for Asn-linked complex-type oligosaccharides.

The crystallization of PELa in complex with trimannose results in infinite lectin chains in the crystal with one carbohydrate ligand bridging two lectin dimers through its terminal nonreducing mannose residues (Fig. 5*A*). Such trimannose bridging has already been observed in the crystal of snowdrop agglutinin (37) and bacterial lectin (38) but not in legume lectins. The only other structures of cross-linked legume lectin have been obtained with galactose-specific soybean agglutinin complexed with biantennary blood group I antigen and analogs (39). In PELa, the conformation of the bridging trimannoside is very extended and drastically different from the folded shape previously observed in other legume lectin complexes (20, 33, 34) as displayed in Fig. 6*E* and Table 4. Interestingly, the conformational change is not due to a rotation around the ω angle, which always adopts a *gauche-gauche* conformation in the different legume lectins, but around the Ψ angle that is rotated by 90° (Fig. 6, *D* and *E*).

The preference for asymmetrical *N*-glycans with a short 6-arm has been confirmed by a semi-quantitative analysis of the glycan array data performed at several lectin concentrations. No crystals could be obtained to date for the complex between PELa and the asymmetric compound **E**, but the complex with the symmetric compound **H** (heptasaccharide-Asn) gives some clues about this preference. The GlcNAc on the 3-arm establishes contacts in the extended sites +2 and +3 while maintaining a low energy conformation of the linkages involved. In contrast, the binding of the GlcNAc of the 6-arm in site −1 induces a strong conformational distortion with energy cost. In addition, oxygen O4 is not accessible for elongation by a galactose. Oligosaccharides with long 3-arm and short 6-arm would therefore be energetically favored for binding. There is therefore an excellent agreement between glycan array and crystallographic data. However, solution data from ITC are not concordant because both the asymmetric and symmetric glycan bind with the same strong affinity to PELa. Nevertheless, the enthalpy profiles are different, and the asymmetric glycan has a much stronger enthalpy of binding, which confirms that the presence of an extra GlcNAc on the 6-arm is not favorable. The difference in entropy contribution between the two oligosaccharides is more difficult to explain. Possible reasons for such differences in entropy could be the trapping/release of water molecules on the protein surface. This work therefore exemplifies one of the cases where the physicochemical state of the ligand, *i.e.* solution state or attached to a surface, can influence its affinity for a receptor.

Acknowledgments—The glycan microarray analysis was provided by the Consortium for Functional Glycomics funded by National Institutes of Health Grant GM62116 from NIGMS. We acknowledge the European Synchrotron Radiation Facility for provision of synchrotron radiation facilities, and we are grateful for the assistance in using beamline BM30A.

REFERENCES

1. Sharon, N., and Lis, H. (1990) Legume lectins. a large family of homologous proteins. *FASEB J.* **4,** 3198–3208
2. Sharon, N., and Lis, H. (1995) Lectins. Proteins with a sweet tooth. Functions in cell recognition. *Essays Biochem.* **30,** 59–75
3. Rüdiger, H., Siebert, H. C., Solís, D., Jiménez-Barbero, J., Romero, A., von der Lieth, C. W., Diaz-Mariño, T., and Gabius, H. J. (2000) Medicinal chemistry based on the sugar code. Fundamentals of lectinology and experimental strategies with lectins as targets. *Curr. Med. Chem.* **7,** 389–416
4. Rüdiger, H. (1998) Plant lectins. More than just tools for glycoscientists. Occurrence, structure, and possible functions of plant lectins. *Acta Anat.* **161,** 130–152
5. Peumans, W. J., and Van Damme, E. J. (1995) Lectins as plant defense proteins. *Plant Physiol.* **109,** 347–352
6. Hirsch, A. M. (1999) Role of lectins (and rhizobial exopolysaccharides) in legume nodulation. *Curr. Opin. Plant Biol.* **2,** 320–326
7. Delatorre, P., Rocha, B. A., Souza, E. P., Oliveira, T. M., Bezerra, G. A., Moreno, F. B., Freitas, B. T., Santi-Gadelha, T., Sampaio, A. H., Azevedo, W. F., Jr., and Cavada, B. S. (2007) Structure of a lectin from *Canavalia gladiata* seeds. New structural insights for old molecules. *BMC Struct. Biol.* **7,** 52
8. Loris, R., Hamelryck, T., Bouckaert, J., and Wyns, L. (1998) Legume lectin structure. *Biochim. Biophys. Acta* **1383,** 9–36
9. Srinivas, V. R., Reddy, G. B., Ahmad, N., Swaminathan, C. P., Mitra, N., and Surolia, A. (2001) Legume lectin family, the "natural mutants of the quaternary state," provide insights into the relationship between protein stability and oligomerization. *Biochim. Biophys. Acta* **1527,** 102–111
10. Sharma, V., and Surolia, A. (1997) Analyses of carbohydrate recognition by legume lectins. Size of the combining site loops and their primary specificity. *J. Mol. Biol.* **267,** 433–445
11. Young, N. M., and Oomen, R. P. (1992) Analysis of sequence variation among legume lectins. A ring of hypervariable residues forms the perimeter of the carbohydrate-binding site. *J. Mol. Biol.* **228,** 924–934
12. Ambrosi, M., Cameron, N. R., and Davis, B. G. (2005) Lectins. Tools for the molecular understanding of the glycocode. *Org. Biomol. Chem.* **3,** 1593–1608
13. Dam, T. K., and Brewer, C. F. (2002) Thermodynamic studies of lectin-carbohydrate interactions by isothermal titration calorimetry. *Chem. Rev.* **102,** 387–429
14. Dam, T. K., Oscarson, S., and Brewer, C. F. (1998) Thermodynamics of binding of the core trimannoside of asparagine-linked carbohydrates and deoxy analogs to *Dioclea grandiflora* lectin. *J. Biol. Chem.* **273,** 32812–32817
15. Williams, B. A., Chervenak, M. C., and Toone, E. J. (1992) Energetics of lectin-carbohydrate binding. A microcalorimetric investigation of concanavalin A-oligomannoside complexation. *J. Biol. Chem.* **267,** 22907–22911
16. Cavada, B. S., Moreira, R. A., Oliveira, J. T., and Grangeiro, T. B. (1993) Primary structures and functions of plant lectins. *R. Bras. Fisol. Veg.* **5,** 193–201
17. Buts, L., Garcia-Pino, A., Imberty, A., Amiot, N., Boons, G. J., Beeckmans, S., Versées, W., Wyns, L., and Loris, R. (2006) Structural basis for the recognition of complex-type biantennary oligosaccharides by *Pterocarpus angolensis* lectin. *FEBS J.* **273,** 2407–2420
18. Garcia-Pino, A., Buts, L., Wyns, L., Imberty, A., and Loris, R. (2007) How a plant lectin recognizes high mannose oligosaccharides. *Plant Physiol.* **144,** 1733–1741
19. Loris, R., Imberty, A., Beeckmans, S., Van Driessche, E., Read, J. S., Bouckaert, J., De Greve, H., Buts, L., and Wyns, L. (2003) Crystal structure of *Pterocarpus angolensis* lectin in complex with glucose, sucrose, and turanose. *J. Biol. Chem.* **278,** 16297–16303
20. Loris, R., Van Walle, I., De Greve, H., Beeckmans, S., Deboeck, F., Wyns, L., and Bouckaert, J. (2004) Structural basis of oligomannose recognition by the *Pterocarpus angolensis* seed lectin. *J. Mol. Biol.* **335,** 1227–1240
21. Lorenzi, H. (1998) *Árvores Brasileiras: Manual de Identificação e Cultivo de Plantas Arbóreas Nativas do Brasil*, Plantarum, Nova Odessa, Brazil
22. Kajihara, Y., Suzuki, Y., Yamamoto, N., Sasaki, K., Sakakibara, T., and Juneja, L. R. (2004) Prompt chemoenzymatic synthesis of diverse complex-type oligosaccharides and its application to the solid-phase synthesis of a glycopeptide with Asn-linked sialyl-undeca- and asialo-nonasaccharides. *Chemistry* **10,** 971–985
23. Moreira, A., and Perrone, J. C. (1977) Purification and partial characterization of a lectin from *Phaseolus vulgaris*. *Plant Physiol.* **59,** 783–787
24. Wiseman, T., Williston, S., Brandts, J. F., and Lin, L. N. (1989) Rapid measurement of binding constants and heats of binding using a new titration calorimeter. *Anal. Biochem.* **179,** 131–137
25. McCoy, A. J., Grosse-Kunstleve, R. W., Adams, P. D., Winn, M. D., Storoni, L. C., and Read, R. J. (2007) Phaser crystallographic software. *J. Appl. Crystallogr.* **40,** 658–674
26. Murshudov, G. N., Vagin, A. A., and Dodson, E. J. (1997) Refinement of macromolecular structures by the maximum-likelihood method. *Acta Crystallogr. D. Biol. Crystallogr.* **53,** 240–255
27. Emsley, P., Lohkamp, B., Scott, W. G., and Cowtan, K. (2010) Features and development of Coot. *Acta Crystallogr. D. Biol. Crystallogr.* **66,** 486–501
28. Wallace, A. C., Laskowski, R. A., and Thornton, J. M. (1995) LIGPLOT. A program to generate schematic diagrams of protein-ligand interactions. *Protein Eng.* **8,** 127–134
29. Seko, A., Koketsu, M., Nishizono, M., Enoki, Y., Ibrahim, H. R., Juneja, L. R., Kim, M., and Yamamoto, T. (1997) Occurrence of a sialylglycopeptide and free sialylglycans in hen's egg yolk. *Biochim. Biophys. Acta* **1335,** 23–32
30. Gourdine, J. P., Cioci, G., Miguet, L., Unverzagt, C., Silva, D. V., Varrot, A., Gautier, C., Smith-Ravin, E. J., and Imberty, A. (2008) High affinity interaction between a bivalve C-type lectin and a biantennary complex-type *N*-glycan revealed by crystallography and microcalorimetry. *J. Biol. Chem.* **283,** 30112–30120
31. Mezzato, S., and Unverzagt, C. (2010) Synthesis of an Fmoc-Asn-heptasaccharide building block and its application to chemoenzymatic glycopeptide synthesis. *Carbohydr. Res.* **345,** 1306–1315
32. Derewenda, Z., Yariv, J., Helliwell, J. R., Kalb, A. J., Dodson, E. J., Papiz, M. Z., Wan, T., and Campbell, J. (1989) The structure of the saccharide-binding site of concanavalin A. *EMBO J.* **8,** 2189–2193
33. Loris, R., Maes, D., Poortmans, F., Wyns, L., and Bouckaert, J. (1996) A structure of the complex between concanavalin A and methyl-3,6-di-*O*-(α-D-mannopyranosyl)-α-D-mannopyranoside reveals two binding modes. *J. Biol. Chem.* **271,** 30614–30618
34. Rozwarski, D. A., Swami, B. M., Brewer, C. F., and Sacchettini, J. C. (1998) Crystal structure of the lectin from *Dioclea grandiflora* complexed with core trimannoside of asparagine-linked carbohydrates. *J. Biol. Chem.* **273,** 32818–32825
35. Imberty, A., Delage, M. M., Bourne, Y., Cambillau, C., and Pérez, S. (1991) Data bank of three-dimensional structures of disaccharides: Part II, *N*-acetyllactosaminic type *N*-glycans. Comparison with the crystal structure of a biantennary octasaccharide. *Glyconconj. J.* **8,** 456–483
36. Moothoo, D. N., and Naismith, J. H. (1998) Concanavalin A distorts the β-GlcNAc-(1→2)-Man linkage of β-GlcNAc-(1→2)-α-Man-(1→3)-[β-GlcNAc-(1→2)-α-Man-(1→6)]-Man upon binding. *Glycobiology* **8,** 173–181
37. Wright, C. S., and Hester, G. (1996) The 2.0-Å structure of a cross-linked complex between snowdrop lectin and a branched mannopentaose. Evidence for two unique binding modes. *Structure* **4,** 1339–1352
38. Lameignere, E., Shiao, T. C., Roy, R., Wimmerova, M., Dubreuil, F., Varrot, A., and Imberty, A. (2010) Structural basis of the affinity for oligomannosides and analogs displayed by BC2L-A, a *Burkholderia cenocepacia* soluble lectin. *Glycobiology* **20,** 87–98
39. Olsen, L. R., Dessen, A., Gupta, D., Sabesan, S., Sacchettini, J. C., and Brewer, C. F. (1997) X-ray crystallographic studies of unique cross-linked lattices between four isomeric biantennary oligosaccharides and soybean agglutinin. *Biochemistry* **36,** 15073–15080
40. Gouet, P., Courcelle, E., Stuart, D. I., and Métoz, F. (1999) ESPript. Analysis of multiple sequence alignments in PostScript. *Bioinformatics* **15,** 305–308